AIAA 2000-0624

A New Eddy Dissipation Rate Formulation for the Terminal Area PBL Prediction System (TAPPS)

Joseph J. Charney, Michael L. Kaplan,
Yuh-Lang Lin, and Karl D. Pfeiffer
North Carolina State University
Raleigh, NC

38th Aerospace Sciences Meeting & Exhibit
January 10-13, 2000 / Reno, NV

A NEW EDDY DISSIPATION RATE FORMULATION FOR THE TERMINAL AREA PBL PREDICTION SYSTEM (TAPPS)

Joseph J. Charney[‡], Michael L. Kaplan[†], Yuh-Lang Lin*, and Karl D. Pfeiffer[§]

Department of Marine, Earth, and Atmospheric Science
North Carolina State University
Raleigh, North Carolina 27695-8208

ABSTRACT

The TAPPS employs the MASS model to produce mesoscale atmospheric simulations in support of the Wake Vortex project at Dallas Fort-Worth International Airport (DFW). A post-processing scheme uses the simulated three-dimensional atmospheric characteristics in the planetary boundary layer (PBL) to calculate the turbulence quantities most important to the dissipation of vortices: turbulent kinetic energy and eddy dissipation rate. TAPPS will ultimately be employed to enhance terminal area productivity by providing weather forecasts for the Aircraft Vortex Spacing System (AVOSS). The post-processing scheme utilizes experimental data and similarity theory to determine the turbulence quantities from the simulated horizontal wind field and stability characteristics of the atmosphere. Characteristic PBL quantities important to these calculations are determined based on formulations from the Blackadar PBL parameterization, which is regularly employed in the MASS model to account for PBL processes in mesoscale simulations. The TAPPS forecasts are verified against high-resolution observations of the horizontal winds at DFW. Statistical assessments of the error in the wind forecasts suggest that TAPPS captures the essential features of the horizontal winds with considerable skill. Additionally, the turbulence quantities produced by the post-processor are shown to compare favorably with corresponding tower observations.

* Professor

† Visiting Professor

‡ Visiting Assistant Professor

§ Graduate Research Assistant

INTRODUCTION

The Terminal Area PBL Prediction System (TAPPS) is being developed to produce meso-β scale simulations of meteorological conditions in support of the Wake Vortex project at Dallas Fort-Worth International Airport (DFW).[1] The centerpiece of TAPPS is the Mesoscale Atmospheric Simulation System (MASS)[2], a mesoscale numerical weather prediction model that provides real time, operational simulations of the planetary boundary layer (PBL) conditions in the DFW area. TAPPS will ultimately be employed to enhance terminal area productivity by providing weather forecasts for the Aircraft Vortex Spacing System (AVOSS).[3,4] The Wake Vortex project in general and AVOSS in particular is designed to, at a given terminal, assess the wake vortex drift and dissipation under varying weather conditions, and compute the optimal safe spacing for landing commercial aircraft.

This study will focus upon the overall performance of the TAPPS system as well as presenting recent enhancements in the post-processing system. The post-processor has been developed by the Department of Marine, Earth, and Atmospheric Science at the North Carolina State University to compute the predictive quantities from the TAPPS simulations required by AVOSS. The scheme employs the simulated three-dimensional winds, thermal structure, and moisture characteristics of the atmosphere to calculate the turbulence-related variables considered most important to the dissipation of vortices: the turbulent kinetic energy (TKE) and eddy dissipation rate (EDR).[1]

MASS/TAPPS MODEL CHARACTERISTICS

Hydrostatic primitive equation model
3-D primitive equations for u, v, T, q, and p
Cartesian grid on a polar stereographic map
σ_p terrain-following vertical coordinate system
One-way interactive nested grid system
Time-dependent lateral boundary conditions
First guess provided by large scale gridded analyses
Reanalysis of rawinsonde, surface, and asynoptic data using a 3-D optimum interpolation scheme
Blackadar PBL scheme
Surface energy budget
Prognostic equations for cloud water, ice, rain water, and snow
Convective parameterization scheme
Post-processing system to compute AVOSS input quantities

POST-PROCESSING SYSTEM

In order for AVOSS to effectively predict the drift and dissipation of vortices in the approach corridor of DFW, it is necessary for the post-processor to provide highly-detailed forecasts of winds, particularly the cross-runway (U) component, from the TAPPS simulations. Time-height cross-sections of the winds are computed by the system with a temporal resolution of 30 minutes, and a vertical spacing of 15m between the surface and 1000m. The variance and the shear of these winds are also very important for AVOSS, and must be computed with precision. Finally, in order to assess vortex dissipation, diagnostics are computed that evaluate the growth, dissipation, and magnitude of the turbulence.

The current version of the TAPPS post-processor employs the model winds, temperature, and moisture fields in conjunction with a first-order closure scheme developed by Han et al. to calculate the EDR and TKE for AVOSS.[1] The scheme utilizes a series of equations developed from experimental data and similarity scaling to determine the EDR and TKE from observations of the three-dimensional wind field and the moist thermodynamic stability characteristics of the atmosphere.[5] The scheme assumes that the PBL has two regimes: 1) neutral and stable, and 2) unstable.

For a statically stable or neutral PBL, the scheme divides the results into two layers. For the surface layer, which is defined as ($z \le 0.1h$), where z is the height above the ground and h is the PBL height, the EDR (ε) is given by:

$$\varepsilon = \frac{u_*^2}{kz}\left(1.24 + 4.3\frac{z}{L}\right), \qquad (1)$$

where u_* is the friction velocity, k ~ 0.4 is the von Karman constant, and L is the Monin-Obukhov length scale. Above the surface layer,

$$\varepsilon = \frac{u_*^2}{kz}\left(1.24 + 4.3\frac{z}{L}\right)\left(1 - 0.85\frac{z}{h}\right)^{1.5}. \qquad (2)$$

For a statically unstable PBL, in which a convective regime dominated by buoyancy prevails, the EDR is calculated as follows:

$$\varepsilon = \frac{u_*^3}{kz}\left(1 + 0.5\left|\frac{z}{L}\right|^{\frac{2}{3}}\right)^{\frac{3}{2}}, \qquad (3)$$

for the surface layer ($z \le 0.1h$). Above the surface layer in a convective regime, turbulent processes arising due to the statically unstable conditions lead to well-mixed atmospheric conditions up through the top of the PBL. In this so-called *mixed layer*, the EDR becomes:

$$\varepsilon = \frac{w_*^3}{h}\left(0.8 - 0.3\left|\frac{z}{h}\right|\right), \qquad (4)$$

where w_* is the convective velocity scale.

The formulation for the TKE (e) follows a similar framework. For a statically stable or neutral PBL, the scheme divides the results into two layers. For the surface layer ($z \le 0.1h$),

$$e = 6u_*^2, \qquad (5)$$

and above the surface layer,

$$e = 6u_*^2\left(1 - \frac{z}{h}\right)^{1.75}, \qquad (6)$$

For a statically unstable PBL, the TKE is calculated as follows:

$$e = 0.36 w_*^2 + 0.85 u_*^2 \left(1 - 3\frac{z}{L}\right)^{\frac{2}{3}}, \qquad (7)$$

for the surface layer ($z \le 0.1h$), and:

$$e = \left(0.36 + 0.9\left(\frac{z}{h}\right)^{\frac{2}{3}}\left(1 - 0.8\frac{z}{h}\right)^2\right) w_*^2, \quad (8)$$

for the mixed layer.

There are three quantities in the above equations that must be defined before this scheme can be applied to the simulated fields: the PBL height (h), the friction velocity (u_*), and the convective velocity scale (w_*). In previous versions of the post-processor, these quantities were derived by first evaluating the turbulent character of the PBL from the resolved model winds and then inferring the other quantities based on as series of empirical relationships between the TKE and the generally observed characteristics of the PBL. However, Eqns. 1-8 were designed to calculate the EDR using wind values taken from tower observations of PBL winds. The resolved winds from a mesoscale atmospheric model (which has a horizontal resolution on the order of 12km) will not, in general, display the same degree of small-scale variability that occurs in tower-based PBL observations. As a result, the model resolved winds will not provide information about the turbulent characteristics of the PBL, and thus will tend to yield values for EDR and TKE that are significantly smaller than those calculated from observed winds.

In order to overcome this potentially serious limitation, the post-processing scheme has been revised such that the EDR and TKE calculations are more representative of the background turbulence than the resolved mesoscale model fields. This was accomplished by using formulations from the Blackadar PBL parameterization, which is employed within MASS to account for sub-grid scale PBL processes that cannot be explicitly calculated by the model due to its resolution.[6,7] By using the Blackadar parameterization, representations for u_*, h, and w_* that are not wholly dependent upon the resolved model winds can be obtained.

Perhaps the most important of these modifications to the overall performance of the post-processor is the formulation for u_*. Within the Blackadar PBL parameterization, u_* is calculated by using a scheme that separates PBL conditions into 4 regimes: (1) the stable regime, (2) the damped mechanical turbulence regime, (3) the forced convection regime, and (4) the free convection regime. These regimes are determined by calculating the bulk Richardson number and assessing the buoyant characteristics of the PBL. Then u_* becomes:

$$u_* = \max\left(\frac{kV_a}{\ln\left(\frac{z_a}{z_o}\right) - \Psi_m}, \; u_{*_n}\right). \qquad (9)$$

where V_a is the velocity at the top of the surface layer, z_a is the height of the surface layer, z_o is the roughness length, and Ψ_m is the correction to the log profile of momentum due to deviations from neutral stratification within the various PBL regimes. u_{*_n} is a pre-defined minimum of the friction velocity that is generally used only in the stable regime (regime 1). This parameterization for u_*, which takes into account the background thermodynamic and turbulence characteristics of the simulated atmosphere, provides substantially better information about the turbulent characteristics of the PBL, which in turn leads to more accurate and physically consistent EDR and TKE predictions.

The Blackadar PBL parameterization also includes a formulation for the PBL height (h) in the convective regime (regime 4) based on the buoyancy characteristics of the airmass.[6,7] Outside of the convective regime, an empirical relationship that defines h for a stationary, neutral PBL is employed.[5]

The convective velocity scale is represented by:

$$w_* = \left(\frac{g}{T_o}\overline{\left(w'\theta_v'\right)_s} h\right)^{\frac{1}{2}}. \qquad (10)$$

where g is the gravitational acceleration, T_o is the reference temperature, and $\overline{\left(w'\theta_v'\right)_s}$ is the mean surface heat flux. Since the surface heating parameterization within the MASS model accounts for the shortwave radiative heating effects, a representation of the surface heat flux that is physically consistent with the u_* and h calculations can be used. By incorporating this value into Eqn. 10, the convective velocity scale will likewise

be consistent with the rest of the input into the EDR and TKE scheme.

PARAMETERS OF TAPPS DFW FORECASTS

Horizontal grid resolution = 12km
Vertical grid resolution = 56 levels between 5m and 16,000m
Length of forecast = 21 hours
Forecast frequency = 2 per day, starting at 0300 UTC and 1500 UTC
Forecast time required = ~3 hours
Domain size = ~ 720 km X 720 km square centered on DFW
AVOSS products = U, V, U-variance, V-variance, U-shear, θ_v, EDR, and TKE
Vertical resolution of AVOSS products = 68 vertical levels from 0 to 1000m at 15m intervals

TAPPS RESULTS

In order to assess the performance of the post-processor, it is necessary to first verify that the model winds are in agreement with observations. Figs. 1-2 show comparisons between the TAPPS simulated U (cross-runway) and V (along-runway) components of the horizontal winds and the wind consensus profiles produced by MIT Lincoln Labs from tower, profiler, lidar, and other *in situ* observations at DFW (referred to as the AVOSS Winds Analysis System, or AWAS).[8] Fig. 1 shows time-height cross sections of the two wind components for 2 November, 1999, while Fig 2 corresponds to 19 November, 1999. These two cases were chosen because both situations involve the passage of a synoptic-scale front, which is traditionally a difficult feature for mesoscale models to predict. As evidenced by the sharp reversal in direction of the V-wind components (Figs. 1c,d and 2c,d), TAPPS and the observations both clearly indicate the passage of the fronts in these cases.

It is noteworthy that TAPPS reproduces with some degree of accuracy both the level and magnitude of the wind maximums associated with the approaching fronts. In particular, the agreement between TAPPS and AWAS for the U-wind component maximum on 2 November (Fig. 1a,b) and for the V-component maximum on 19 November (Fig. 2c,d) shows considerable skill. The high degree of agreement between the overall structures in both wind components during the passage of these fronts suggests that TAPPS can reproduce mesoscale features in the horizontal wind fields that are often difficult to replicate. Although not shown here, it is also notable that TAPPS also verifies well in situations where a nocturnal low-level jet (LLJ) is observed by the AWAS. The almost ubiquitous nature of LLJs in the DFW area during much of the year presents a considerable challenge for AVOSS, and that TAPPS regularly captures these features is also encouraging. Furthermore, that TAPPS is providing information about these features some 12 hours *before* they actually occurred, shows in dramatic fashion the utility of these simulations to AVOSS as a whole.

STATISTICAL CALCULATIONS

Bias: $$\frac{\sum_{i=1}^{N}\left\{X_{tapps} - X_{obs}\right\}}{N}$$

Mean Absolute Error = $$\frac{\sum_{i=1}^{N}\left|X_{tapps} - X_{obs}\right|}{N}$$

RMS Error = $$\sqrt{\frac{\sum_{i=1}^{N}\left\{X_{tapps} - X_{obs}\right\}^2}{N}}$$

A statistical error analysis that assesses the overall performance of TAPPS in comparison to AWAS is shown in Fig. 3. These statistics were computed from the differences between TAPPS and AWAS for 28 real-time simulations in November 1999. These simulations were initiated at 0000 UTC on each date. Results were analyzed for every 30-minute time period for which there were both observations and model output, resulting in a sample size on the order of 1300 for each level. For the purpose of understanding these results, it is worth noting that the estimated error in the instruments that provided data for the AWAS profiles is on the order of 1 m/s.[8] The bias statistics suggest that there is little overall bias in the TAPPS predictions, particularly in the lowest levels. Even at the highest levels, the overall bias is less than the estimated errors in the observations.

The mean absolute error (MAB) is on the order of 1.5 m/s in the lowest 500m of the profile, and increases to near 2 m/s at the higher levels. The increase in MAB at the higher levels can be attributed to the typically higher wind speeds in the upper levels, which causes larger magnitude differences should the model develop phase errors in the simulated weather systems. Nevertheless, overall MAB values on the order of 1.5 m/s in the lowest 500m, which is the layer most vital to the performance of AVOSS, is very encouraging. The RMS errors are, as expected, somewhat larger than the mean absolute errors. However, since RMS error calculations are designed to punish particularly large differences between TAPPS and AWAS, RMS errors less than 1 m/s greater than the MAB in all cases suggests that there are few extremely large "misses" during the month.

Finally, Figs. 4 and 5 show an example of TAPPS TKE and EDR predictions respectively at three

different times on 15 November, 1999. The TAPPS profiles are compared against EDR and TKE profiles inferred from 5m and 45m tower observations by using the technique described in Han et al.[5] These profiles show that, in this particular case, TAPPS generated TKE and EDR values that are of the same order of magnitude as those inferred from the tower observations, which is very encouraging. The vertical structure of the quantities is also well represented in the early times in particular (Figs 4a,b and 5a,b), when the PBL was in a stable regime. In the afternoon (4c and 5c), the vertical structure of the EDR and TKE are less comparable, due to disagreements between the TAPPS simulations and the tower observations of EDR and TKE in the convective regime. Nevertheless, the fact that the two techniques agree within an order of magnitude shows a considerable improvement over the techniques that were previously employed as part of the TAPPS system. However, there is clearly a need for more comprehensive statistical comparisons between TAPPS and observations of EDR and TKE. There are plans to start calculating the EDR and TKE by using AWAS and profiler data in the near future, which will provide more comprehensive verification information with which the overall performance of the post-processor can be assessed.

CONCLUSIONS

A new formulation for predicting the evolution of turbulence variables in the PBL from TAPPS simulations has been presented. The physics of the new formulation, which utilizes elements of the Blackadar PBL parameterization to account for the sub-grid scale characteristics necessary to reproduce the details of turbulent flow, was described.

The overall performance of TAPPS was assessed by comparing TAPPS and AWAS horizontal winds in the lowest 1000m of the atmosphere. Examinations of two specific cases as well as an overall statistical assessment of the differences suggested that TAPPS reproduces the salient PBL characteristics in the horizontal wind fields with considerable skill. Comparisons between TAPPS simulation results from the redesigned post-processor and tower-based observations of EDR and TKE showed that the new formulation agreed well with observations for one particular case. Both the temporal evolution and the magnitudes of the simulated quantities were shown to be representative of the conditions at DFW.

ACKNOWLEDGEMENTS

This research is being supported by NASA's Terminal Area Productivity (TAP) program under NASA Cooperative Agreement #NAS 1-99097. The authors would like to thank Dr. Fred H. Proctor for his technical support. Additionally, we would like to acknowledge the support of David A. Hinton, the AVOSS Principal Investigator, and R. Brad Perry, the Reduced Separation and Operations Manager of the NASA-Langley Airborne Systems Competency, for their support and helpful comments on numerous occasions. We would also like to thank J. Al Zak and W. G. Buddy Rodgers for providing us with the DFW tower observations and Han et al. model results used for comparison purposes in this study, as well as for their many valuable comments regarding the performance of the new post-processor.

[1] Kaplan, M. L., R. P. Weglarz, Y.-L. Lin, D. B. Ensley, J. K. Kehoe, and D. S. Decroix, 1999: A terminal area PBL prediction system for DFW. 37th Aerospace Sciences Meeting and Exhibit, Reno, Nevada, AIAA Paper No. 99-0983, 27 pp.

[2] MESO, Inc., 1995: MASS Reference Manuel Version 5.10, 129 pp. [Available from MESO, Inc., 185 Jordan Road, Troy, NY 12180]

[3] Hinton, D. A., 1995: "Aircraft Vortex Spacing System (AVOSS) Conceptual Design." NASA Tech. Memo. No. 110184. [Available from NASA-Langley Research Center, Hampton, Virginia 23681].

[4] Hinton, D. A., J. K. Charnock, D. R. Bagwell, and D. Grigsby, 1999: NASA Aircraft Vortex Spacing System development status. 37th Aerospace Sciences Meeting & Exhibit, Reno, Nevada, AIAA Paper No. 99-0753, 17 pp.

[5] Han, J., S. Shen, S. P. Arya, and Y.-L. Lin, 1999: An estimation of turbulent kinetic energy and energy dissipation rate based on atmospheric boundary layer similarity theory. [Submitted as a NASA contract report]

[6] Blackadar, A. K., 1979: High resolution models of the planetary boundary layer. *Advances in Environmental Science and Engineering*, Vol. 1, No. 1, J. Pfafflin and E. Ziegler, eds., Gordon and Breach, pp. 50-85.

[7] Zhang, D.-L. and R. A. Anthes, 1982: A high resolution model of the planetary boundary layer - sensitivity tests and comparisons with SESAME-79 data. *J. Appl. Meteor.* , **21**, 1594-1609.

[8] Daisey, T. J, R. E. Cole, R. M. Heinrichs, M. P. Matthews, and G. H. Perras, 1998: Aircraft Vortex Spacing System (AVOSS) initial 1997 system deployment at Dallas/Ft. Worth (DFW) airport. NASA Project report NASA/L-3. [Available from the National Technical Information Service, Springfield, Virginia 22161].

a) TAPPS

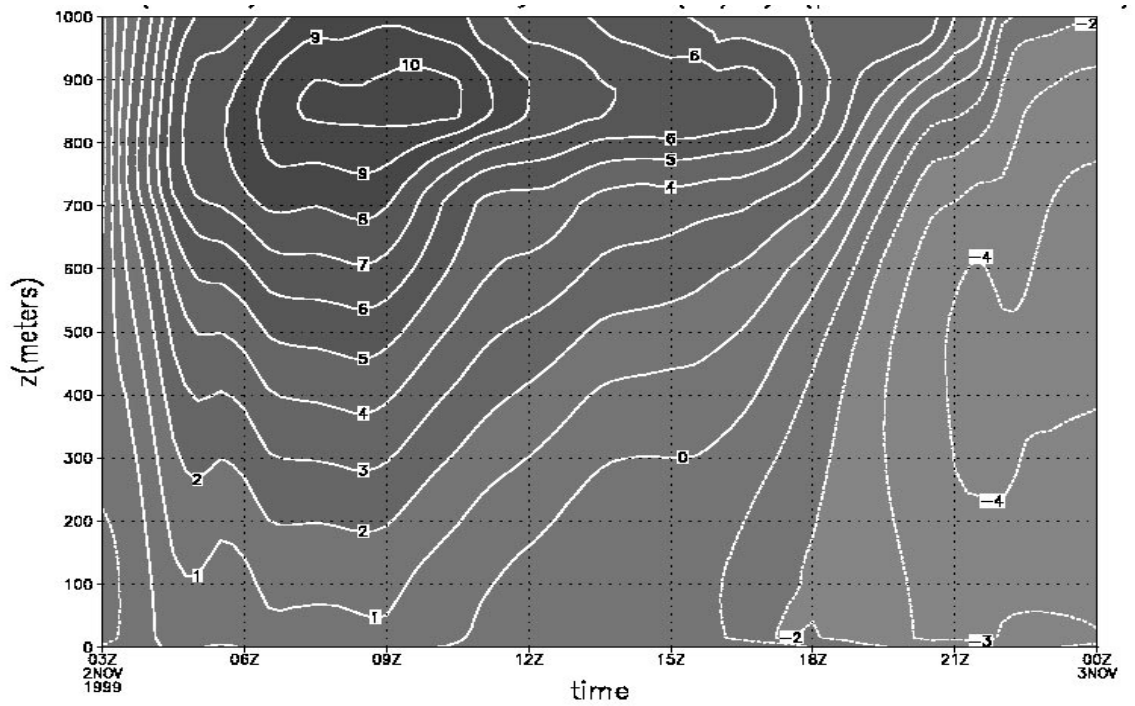

b) AWAS

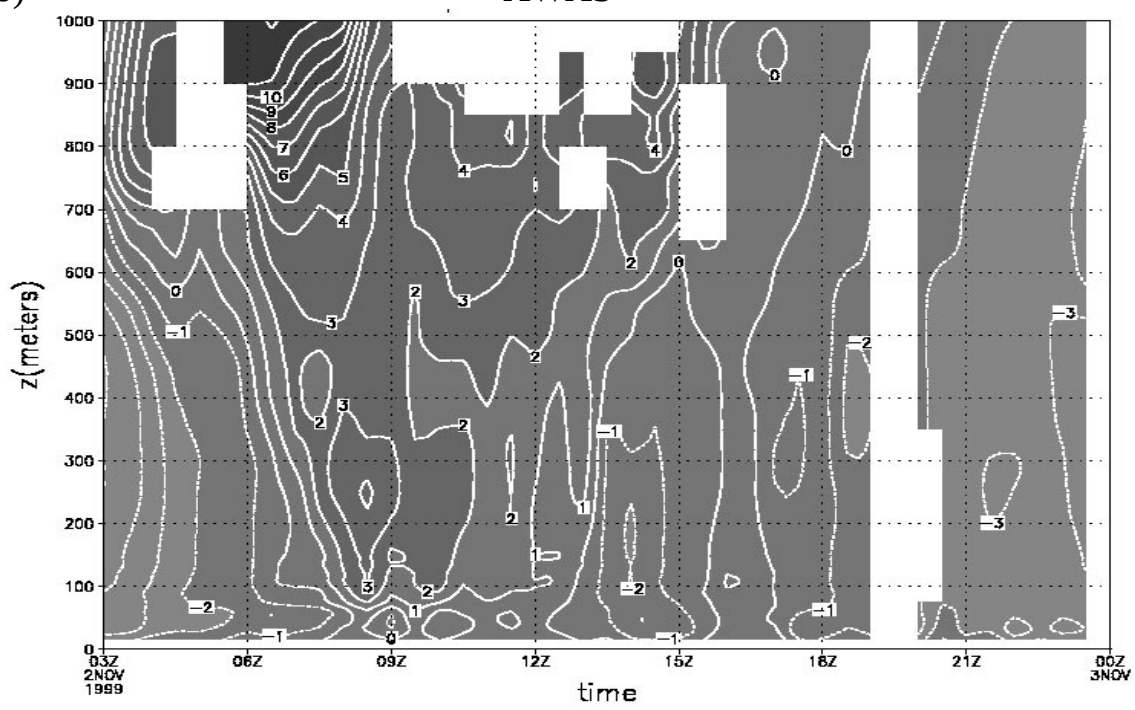

Figure 1: Time-height cross section of the horizontal wind components for 2 November, 1999 at DFW in m/s. a) TAPPS U-component. b) AWAS U-component. c) TAPPS V-component. d) AWAS V-component.

c) TAPPS

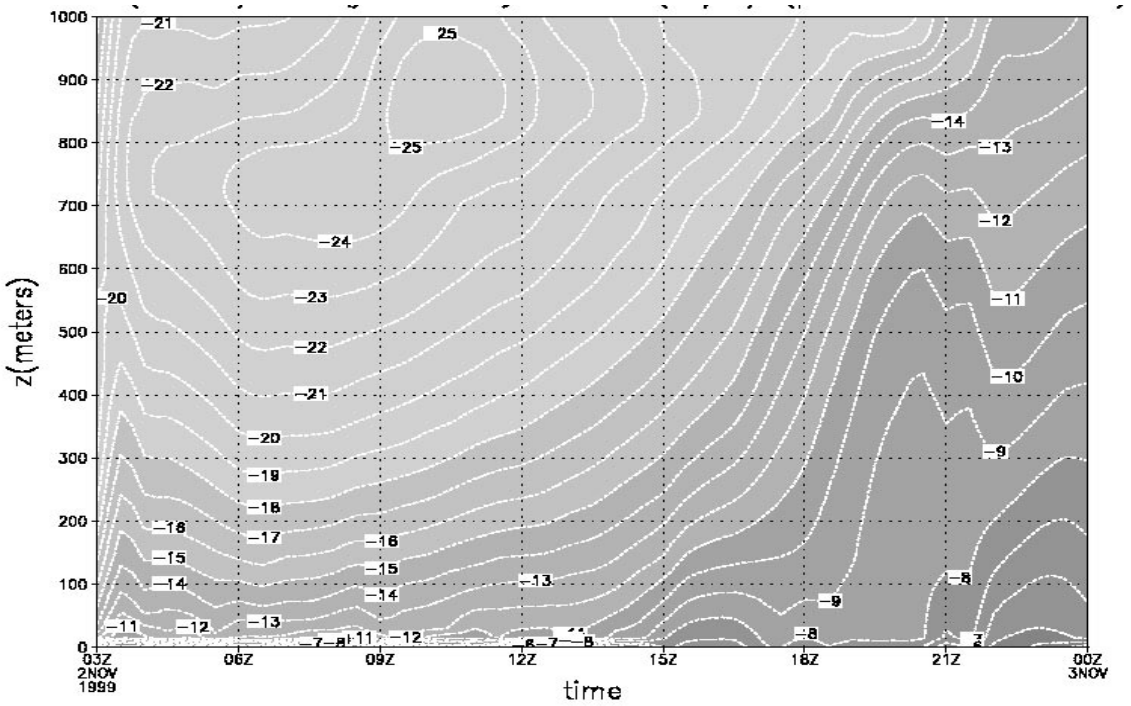

d) AWAS

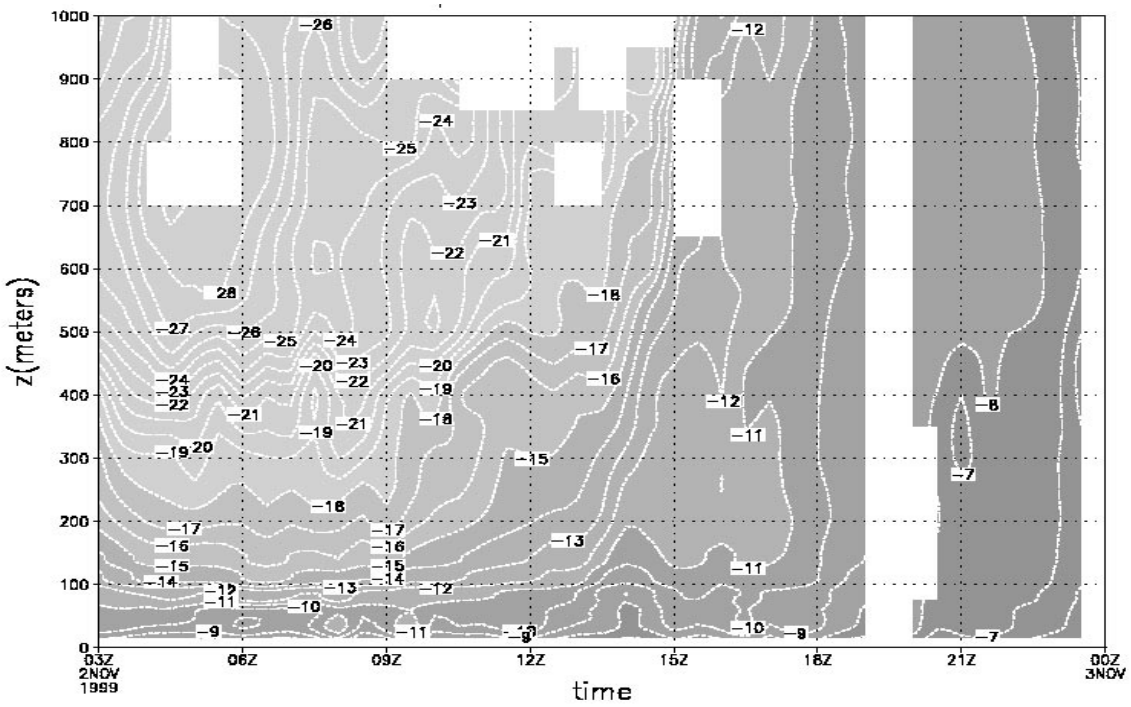

Figure 1: Continued

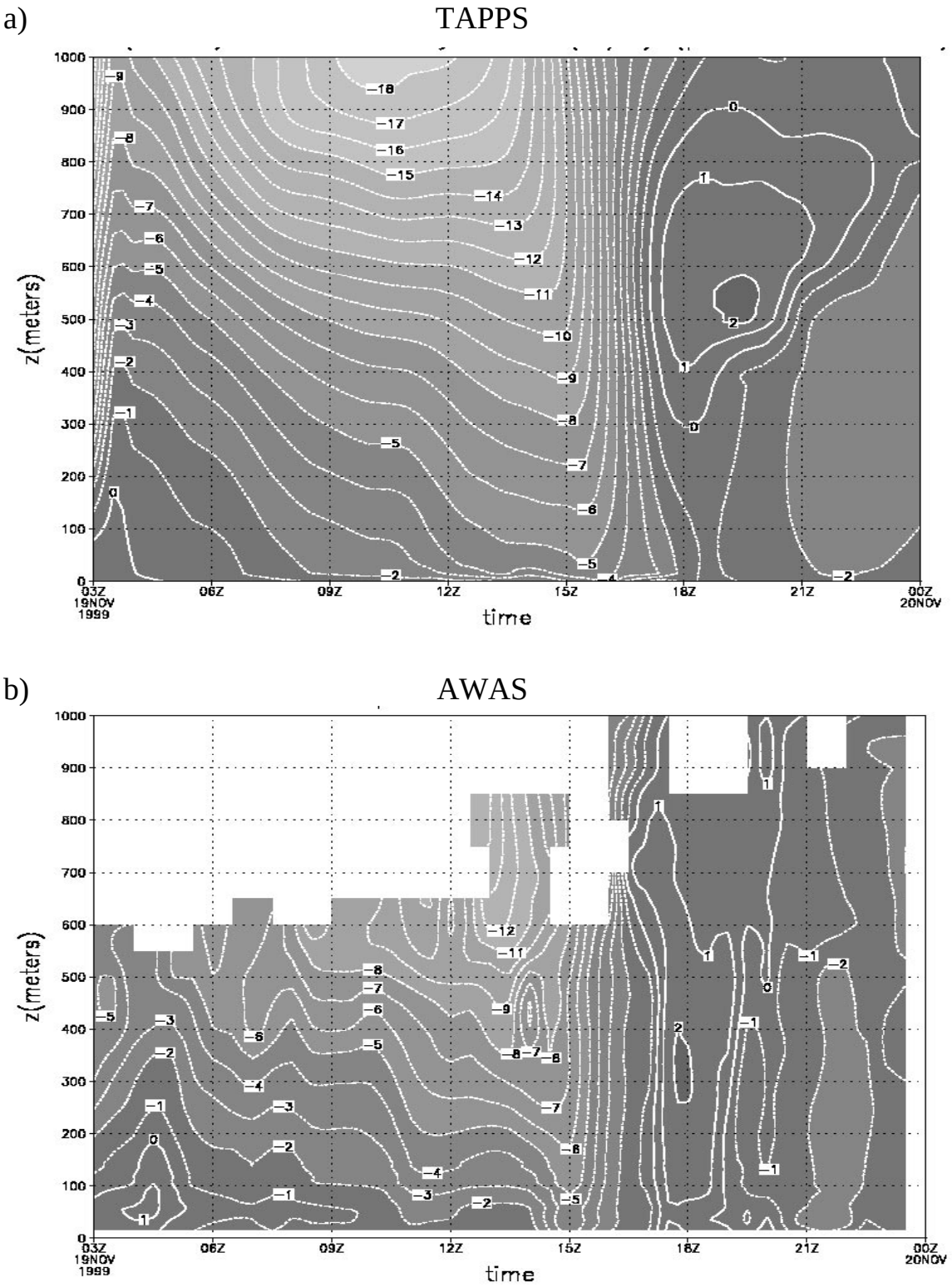

Figure 2: Time-height cross section of the horizontal wind components for 19 November, 1999 at DFW in m/s. a) TAPPS U-component. b) AWAS U-component. c) TAPPS V-component. d) AWAS V-component.

c) TAPPS

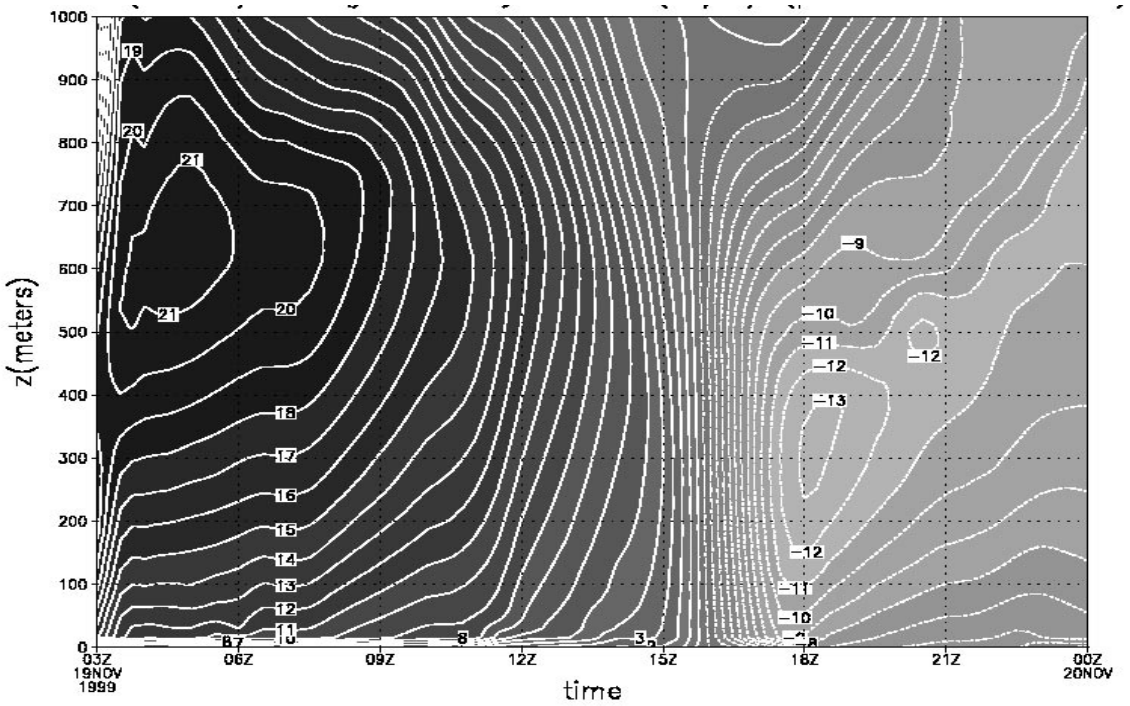

d) AWAS

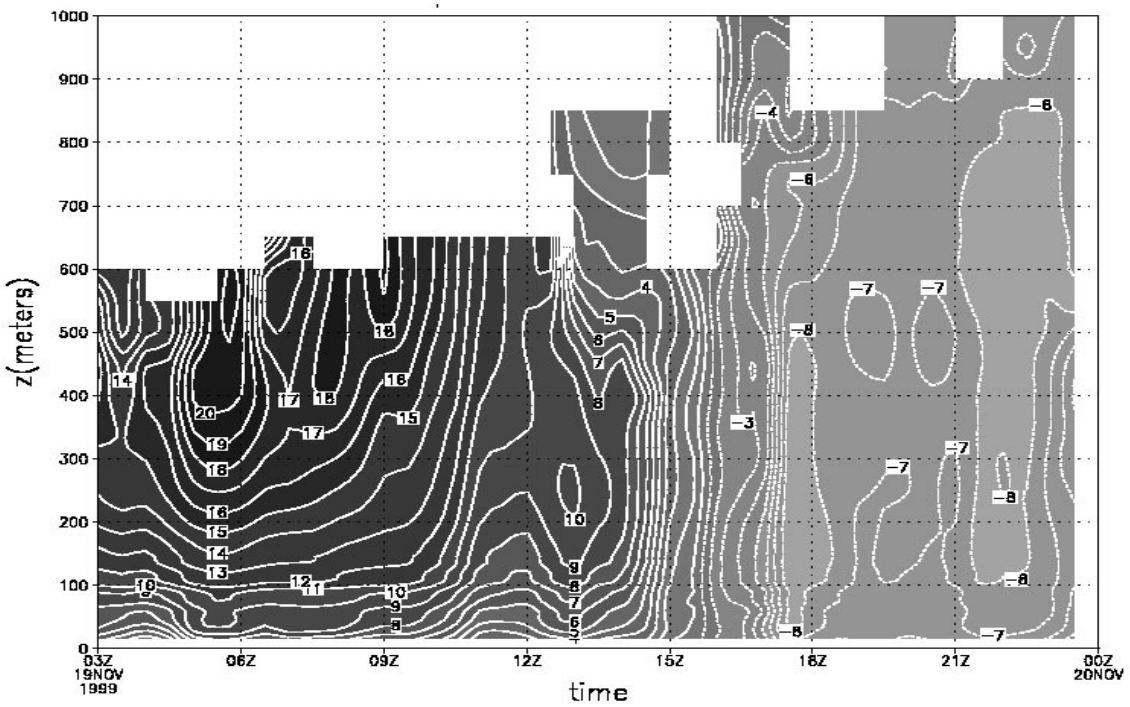

Figure 2: Continued

a) U-wind component

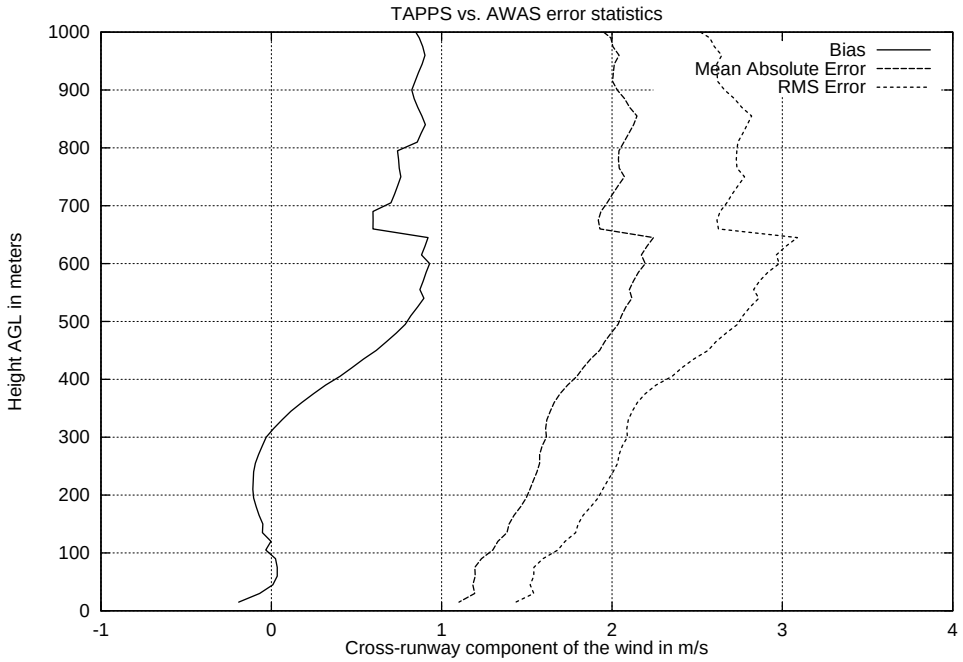

b) V-wind component

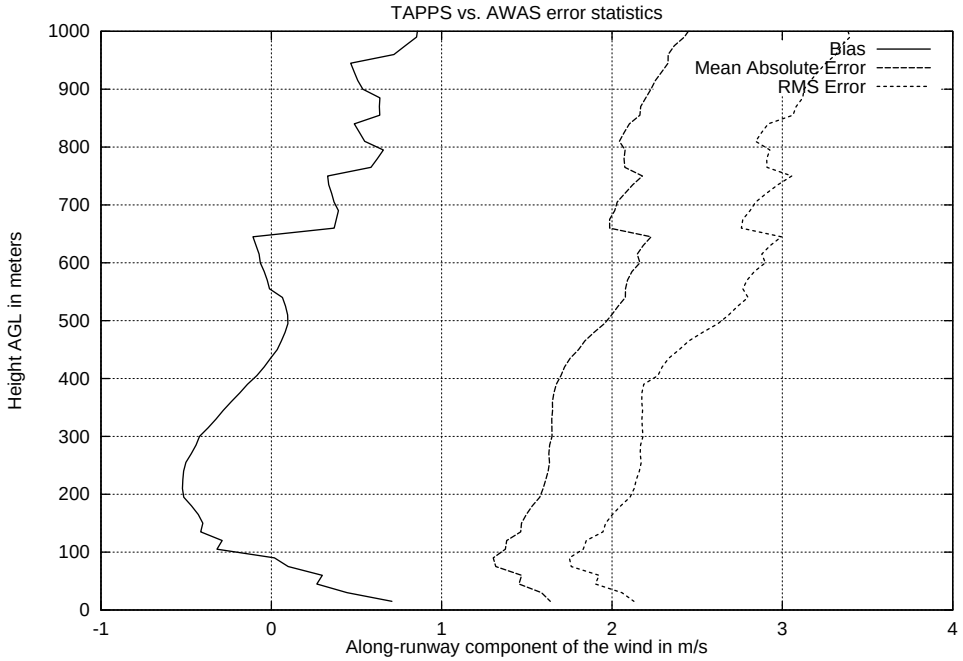

Figure 3: Vertical profiles of bias, mean absolute error, and rms errors between TAPPS and AWAS wind components for the month of November in m/s. a) U-wind component. b) V-wind component.

a) 0600 UTC

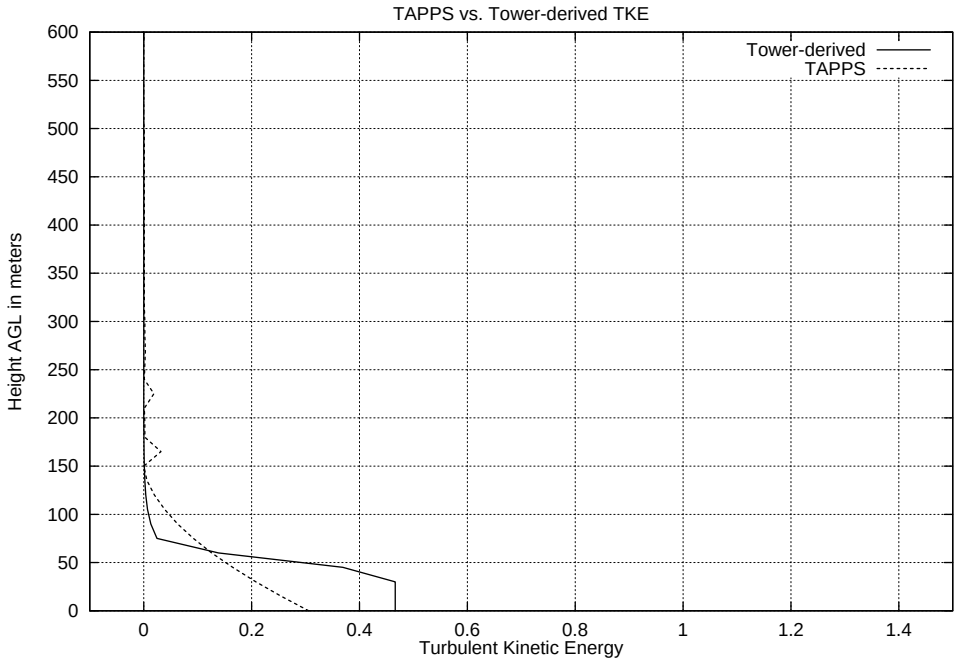

b) 1200 UTC

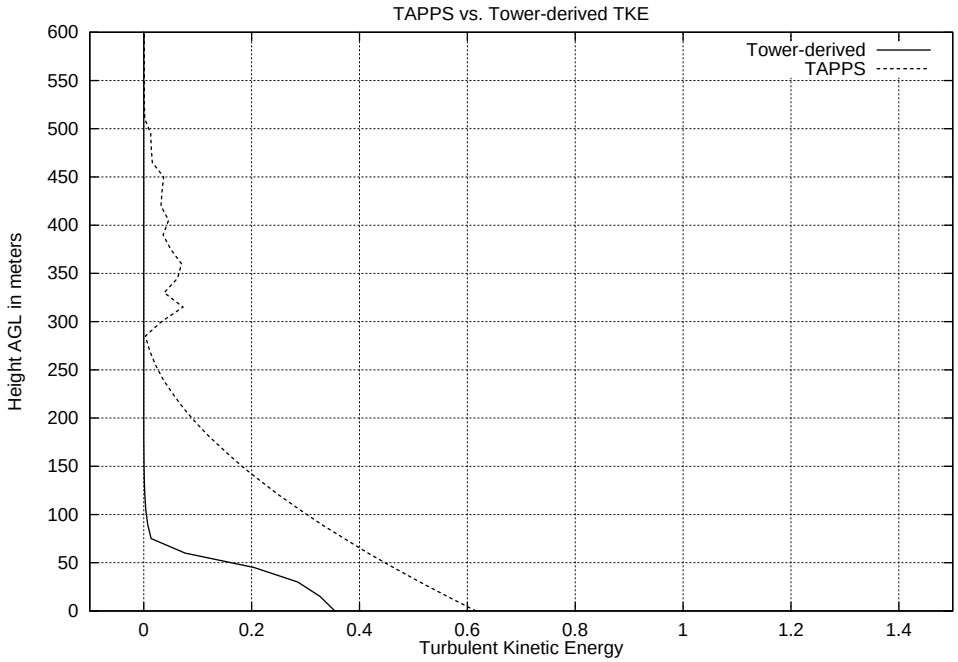

Figure 4: Vertical profiles of TKE from TAPPS and tower observations in m^2/s^3 on 15 November, 1999 at: a) 0600 UTC, b) 1200 UTC, and c) 1900 UTC.

c) 1900 UTC

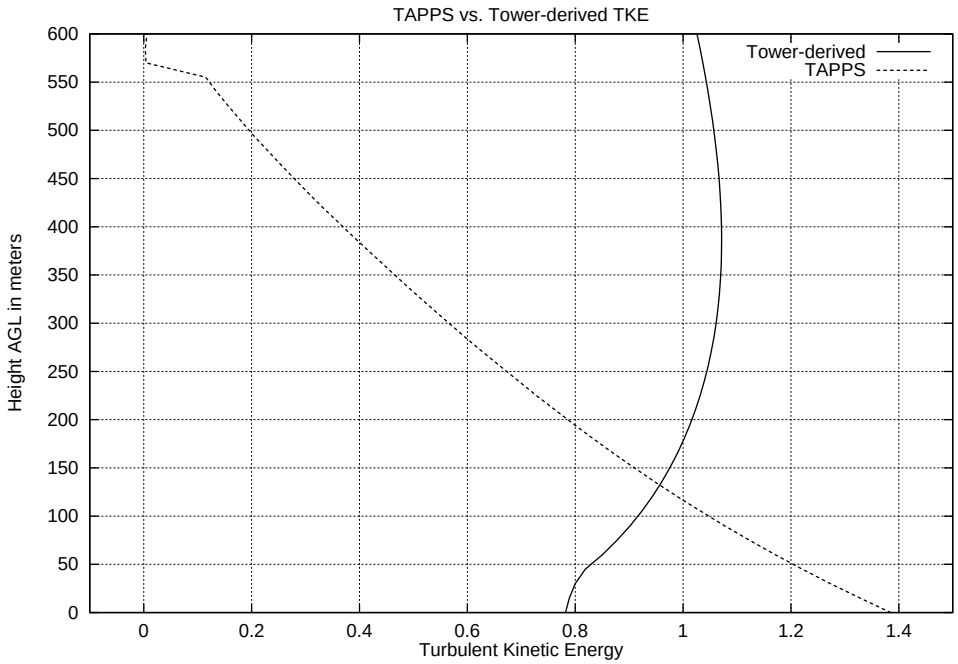

Figure 4: Continued

a) 0600 UTC

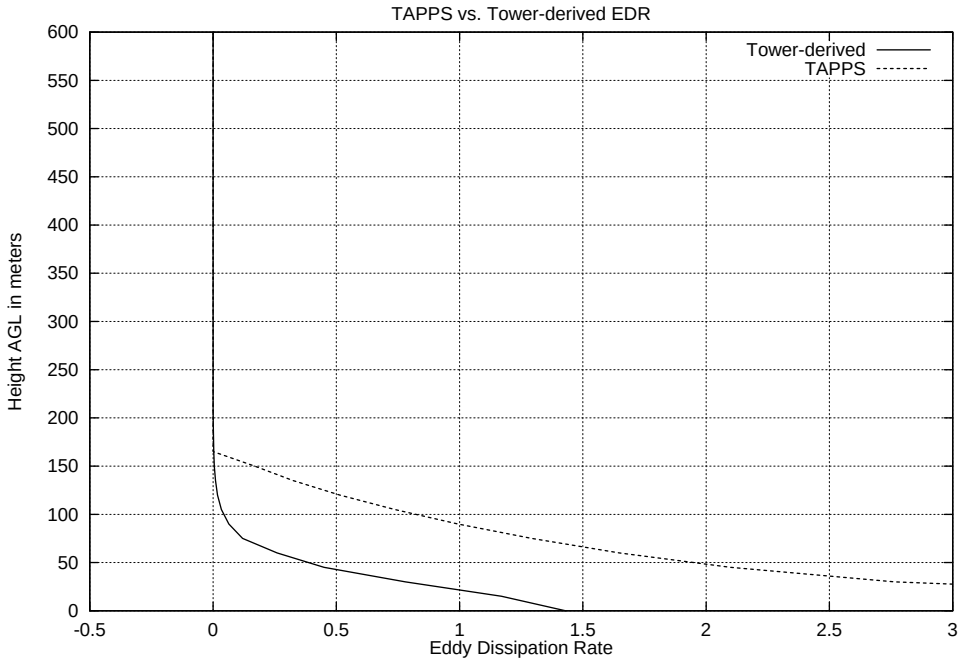

b) 1200 UTC

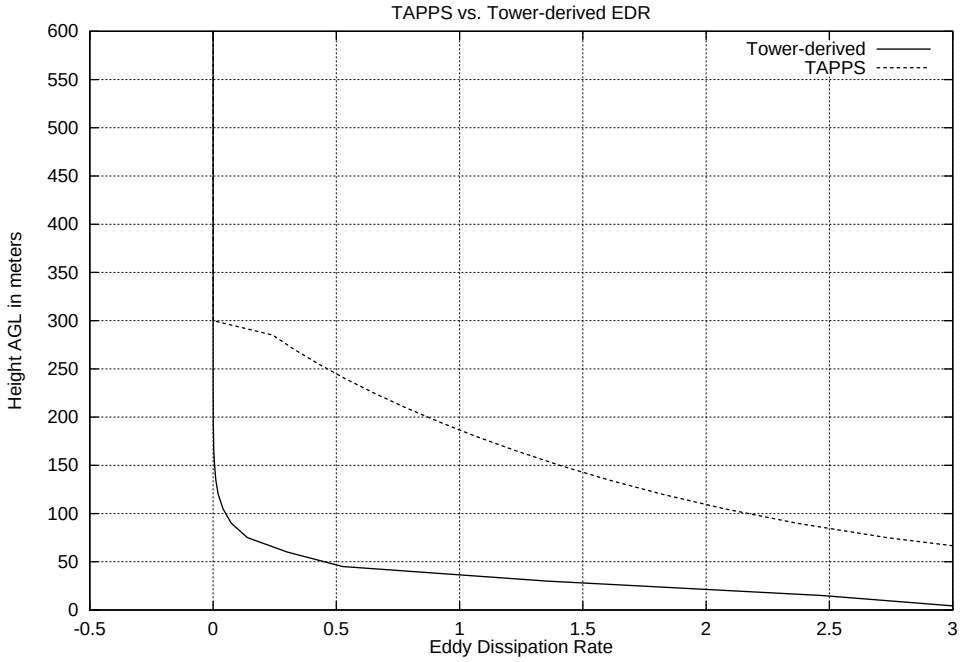

Figure 5: Vertical profiles of EDR from TAPPS and tower observations in $1000*m^2/s^2$ on 15 November, 1999 at: a) 0600 UTC, b) 1200 UTC, and c) 1900 UTC.

c) 1900 UTC

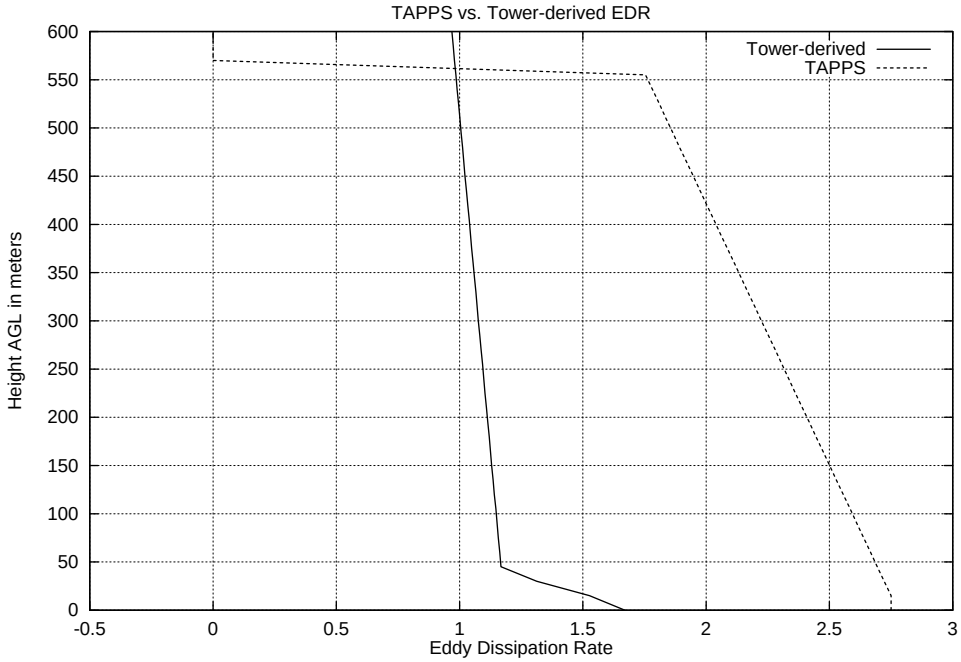

Figure 5: Continued